

Roles of voltage in semi-insulating GaAs photoconductive semiconductor switch*

Hai-Juan Cui(崔海娟)^{1,†}, Hong-Chun Yang(杨宏春)¹, Jun Xu(徐军)¹,
Yu-Ming Yang(杨宇明)², and Zi-Xian Yang(杨子贤)¹

¹School of Physical Electronics, University of Electronic Science and Technology of China, Chengdu 610054, China

²School of Mathematical Sciences, University of Electronic Science and Technology of China, Chengdu 610054, China

(Received 29 August 2016; revised manuscript received 17 October 2016; published online 22 December 2016)

An experimental study of leakage current is presented in a semi-insulating (SI) GaAs photoconductive semiconductor switch (PCSS) with voltages up to 5.8 kV (average field is 19.3 kV/cm). The leakage current increases nonlinearly with the bias voltage increasing from 1.2×10^{-9} A to 3.6×10^{-5} A. Furthermore, the dark resistance, which is characterized as a function of electric field, does not monotonically decrease with the field but displays several distinct regimes. By eliminating the field-dependent drift velocity, the free-electron density n is extracted from the current, and then the critical field for each region of $n(E)$ characteristic of PCSS is obtained. It must be the electric field that provides the free electron with sufficient energy to activate the carrier in the trapped state via multiple physical mechanisms, such as impurity ionization, field-dependent EL2 capture, and impact ionization of donor centers EL10 and EL2. The critical fields calculated from the activation energy of these physical processes accord well with the experimental results. Moreover, agreement between the fitting curve and experimental data of $J(E)$, further confirms that the dark-state characteristics are related to these field-dependent processes. The effects of voltage on SI-GaAs PCSS may give us an insight into its physical mechanism.

Keywords: photoconductive semiconductor switch, leakage current, dark resistance, nonlinear characteristics

PACS: 78.56.-a, 78.30.Fs, 73.20.Hb

DOI: 10.1088/1674-1056/26/1/017804

1. Introduction

Due to the high dark resistivity and breakdown field, a semi-insulating (SI) GaAs photoconductive semiconductor switch (PCSS) is important for pulsed power application.^[1–3] After being charged with voltage, the switch is triggered by the appropriate optical pulse. The PCSS operates in the linear mode with no gain when it is biased with a low voltage. While demonstrating apparent gain with high voltage, the switch runs in lock-on state.^[4–6]

The low leakage current resulting from the high dark resistivity of SI GaAs ensures that high-gain PCSS is capable of sustaining higher electric field before breaking down.^[7–9] Conversely, the increase in leakage current at high voltage can degrade the high resistivity of PCSS,^[7] and then the lifetime,^[10] which is one of the important issues for high-gain PCSS.^[6] Many efforts have been made to study the dark current-voltage characteristics to emphasize performances of GaAs PCSS, such as current oscillations of low frequency,^[11] the effects of different geometries,^[12] and the response time of PCSS at high voltage bias.^[13] Always seen as a constant, the dark resistance has not been taken into account in those researches. In general, the conduction of PCSS is realized by lowering the high resistance, which is obviously changed by the optical energy and voltage.^[14,15] Because the voltage is charged before the optical illumination to trigger the PCSS,

the voltage alone is responsible for the change of the high resistance. Furthermore, for high-power application, the switch voltage does not recover to zero after being irradiated by the optical pulse, but locks at a rather lower voltage until the completion of the discharge.^[2] Because the PCSS is charged with voltage throughout the dynamical process, the roles of voltage need to be analyzed completely to find the physical mechanism of PCSS.

In this work, the accurate measurements on the leakage current of SI-GaAs PCSS are reported with voltages up to 5.8 kV. The dark resistance as a function of electric field shows that there are diverse mechanisms for the PCSS with increasing field. The characteristic of free-electron density extracted from current is integrated with the hot-electron effect to explore the effect of field on the SI-GaAs PCSS in the dark state.

2. Experimental setup

Experimental setup for SI-GaAs PCSS in the dark state is shown in Fig. 1, where R is a current-limiting resistance, R_s is a sample resistance, C is a capacitance used for charging and discharging, and mA and μ A are the ammeters. Because the current in the PCSS oscillates when the bias voltage increases to a certain value, the resistances R and R_s must be non-inductive lest the measurement results are affected. A 3-mm gap lateral PCSS^[16] with opposed-contact arrangement as

*Project supported by the National Natural Science Foundation of China (Grant No. 31470822) and the Advanced Research Foundation of China (Grant Nos. 9140A05030114DZ02068, 9140A07030514DZ02101, and 9140A07010715DZ02001).

†Corresponding author. E-mail: haijuan.cui@uestc.edu.cn

shown in Fig. 2 is formed on a 3-inch diameter, 650- μm thick, and semi-insulating LEC GaAs wafer. The dimensions of the SI-GaAs PCSS are 9 mm (length) \times 6 mm (width) \times 0.6 mm (height). The free electron density, the EL2 density, the resistivity, and mobility of the wafer at zero electric field are, respectively, $n_0 = 2.5 \times 10^7 \text{ cm}^{-3}$, $N_{\text{EL2}} = 1.43 \times 10^{16} \text{ cm}^{-3}$, $\rho = 5 \times 10^7 \Omega\cdot\text{cm}$, and $\mu_0 = 6000 \text{ cm}^2/\text{V}\cdot\text{s}$.

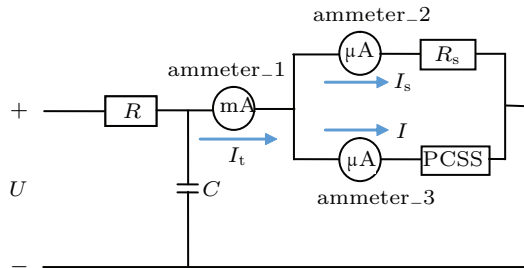


Fig. 1. (color online) Experimental setup for dark-state measurement.

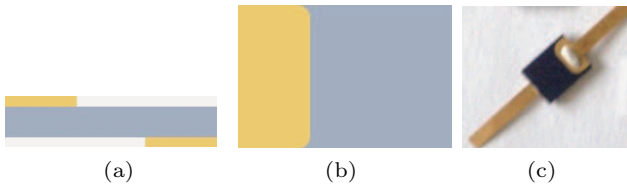


Fig. 2. (color online) (a) Side view, (b) top view, and (c) the photograph of the lateral PCSS.

At room temperature, the leakage currents of three PCSS samples were measured in darkness. The measurements were made when the voltage varied from 20 V to 5800 V, and a milli-ammeter (ammeter_1) and two micro-ammeters (ammeter_2 and ammeter_3) were used to record the currents. Here, the leakage current I of PCSS was recorded by the ammeter_3. Meanwhile, it was checked by subtracting the current of sample resistance I_s from the total current I_t . In order to investigate the current at low voltage closely, a nano-ammeter was used to replace the micro-ammeter in the branch of PCSS to record the leakage current I when the voltage varied from 0.5 V to 60 V. The parameters of the current meters are shown in Table 1. The dark resistance is the bias voltage divided by the current I , where the resistances of the ammeters are small enough to be neglected.

Table 1. Parameters of current meters.

Current meter	Measurement range	Resolution
micro-ammeter	0–199.99 μA	0.01 μA
milli-ammeter	0–19.999 mA	0.001 mA
nano-ammeter	0–19.9 nA	0.1 nA

3. Results and discussion

3.1. Experimental results

Experimental results for three samples are shown in Fig. 3. The currents show almost the same characteristics

when the voltage is below about 2000 V, after which they keep the similar trend despite small divergences. In addition, the current-voltage characteristic of sample 1 with detailed low-voltage data is depicted in Fig. 4 with the log-log coordinate. It can be seen that the current of sample 1 increases from 1.2×10^{-9} A to 3.6×10^{-5} A when the voltage is charged from 0.5 V to 5800 V. All of the current-voltage characteristics in Figs. 3 and 4 consist of four regions. As shown in Fig. 4, they are basically ohmic below about 300 V, while sublinear, accompanied by periodical oscillating current between 300 V and 900 V, then nonlinear respectively above 900 V and above 2000 V.

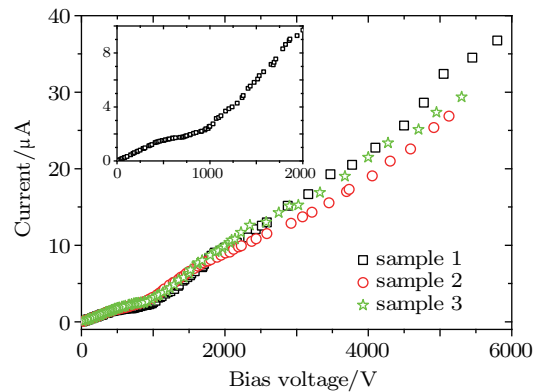


Fig. 3. (color online) Current-voltage characteristic curves of three PCSS samples. The inset shows the current of sample 1 biased with low voltage.

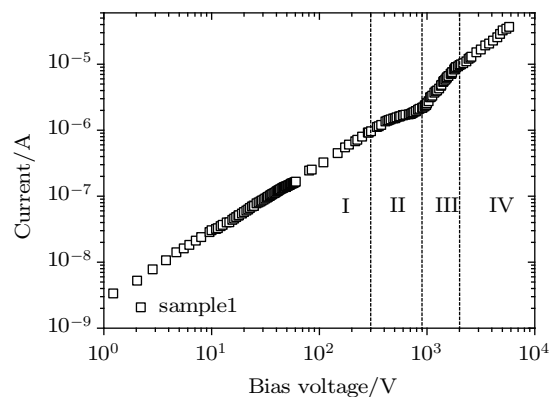


Fig. 4. Current-voltage characteristic curve of sample 1 consisting of four different regions.

The resistances obtained from current data are taken as the dark resistance, because ohmic-contact resistance is negligible in contrast to the dark resistance. Dividing the bias voltage V by the space gap, we obtain the average field E . The dark resistance R_p of sample 1, which is characterized as a function of field E in Fig. 5, does not decrease monotonically with the biased field. On the contrary, the resistance even increases with increasing field. It can be found that the dark resistance-average field characteristic shown in Fig. 5 displays five distinct subsequent regimes. After a constant regime below about 0.5 kV/cm (the inset in Fig. 5), a small decrease

appears in the dark resistance, which has not been detected in current-voltage curves. Above a critical field near 1 kV/cm, the resistance instead increases and then saturates till 3 kV/cm. After that the dark resistance decreases rapidly with an obvious turning point about 7 kV/cm, which is also the divergence point for three samples in Fig. 3. Consequently, the dark resistance is reduced from 335 M Ω at 0.5 kV/cm to 157 M Ω at 19.3 kV/cm.

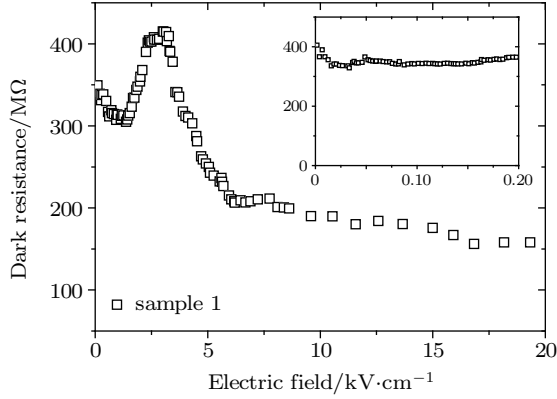


Fig. 5. Dark resistance of sample 1 as a function of electric field. The inset shows the constant resistance at low field.

3.2. Discussion

In the test, SI-GaAs PCSS is biased with the increasing voltage. Gaining energy from the electric field, free electrons in GaAs interact with impurities and donor centers, which causes the free-carrier density to vary with the electric field. The energy of the free electron obtained from the low field can be written as

$$E_1 = Eq\lambda, \quad (1)$$

where q is the unit elementary charge and λ is the mean free path. Under high field the free electron is heated up dramatically, and hence the mobility of GaAs does not keep constant anymore. The gained energy from the high field is expressed as

$$E_h = \frac{3}{2}kT_e, \quad (2)$$

where k is the Boltzmann constant and T_e is the hot-electron temperature, which is higher than lattice temperature T .

Hot-electron temperature T_e can be achieved through the energy-relaxation time τ_e in the relation^[17]

$$Eqv(E) = \frac{3k(T_e - T)}{2\tau_e}, \quad (3)$$

where $v(E)$ is the velocity-field characteristics in GaAs and the energy relaxation time τ_e is assumed to be on the order of 10^{-12} s. The average electron drift velocity is a function of the electric field for GaAs, which exhibits bulk negative differential resistance^[18] because of the high-field transferred electron

effect (TTE). The drift velocity of the electron is related to the applied electric field E by

$$v(E) = \mu(E)E = \frac{\mu_0 E + v_s(E/E_t)^4}{1 + (E/E_t)^4}, \quad (4)$$

where μ_0 is the electron mobility at zero field, v_s is the saturation value of electron drift velocity, and E_t is the critical field of TTE. The threshold field E_t defining the onset of TTE in GaAs should supply the conduction electrons with sufficient energy, 0.35 eV, to be transferred from a high-mobility energy valley to low-mobility satellite valley. According to Eqs. (2)–(4), the threshold field E_t can be expressed as a function of τ_e . Because the critical field of TTE is always near 3.5 kV/cm, E_t is selected to be 3.57 kV/cm with $\tau_e = 4 \times 10^{-12}$ s in Eq. (3) to obtain the temperature of the hot electron.

3.2.1. Free-electron density

In darkness, the current can be written as

$$I(E) = J(E)s = n(E)qv(E)s, \quad (5)$$

where $s = 0.6 \text{ mm} \times 6 \text{ mm}$ is the area of cross section, through which the current flows. For PCSS biased with the field, the increase of current in Eq. (5) can be attributed to the field-dependent free-electron density $n(E)$ and drift velocity $v(E)$. Here the contribution of the diffusion to the current is ignored because of the small free-electron density. In addition, the resistance

$$R(E) = \frac{\rho(E)l}{s} = \frac{l}{n(E)q\mu(E)s} \quad (6)$$

is inversely proportional to the field-dependent mobility $\mu(E)$ and free-electron density $n(E)$. Both the current and resistance are related to free-electron density $n(E)$, therefore the free-electron density $n(E)$ should be extracted from the current by eliminating the drift velocity $v(E)$ of the electron to conduct the research on the dark characteristics of the PCSS.

The densities of the free carrier for three measured PCSS samples are shown in Fig. 6. After an initial constant, the densities increase slightly, decrease, and then increase again. Although the change of free-electron density with electric field is completely opposite to the change of the dark resistance, the critical field for the increase or decrease of the free-carrier density is the same as that of the dark resistance. Moreover, the increase in free-electron density is faster than the decrease in the dark resistance for the electric field higher than 3 kV/cm. It can be found that the free-electron density of sample 1 at 19.3 kV/cm is increased about 12 times in comparison with the initial density, while the dark resistance is reduced only twice.

It is suggested that the fluctuations of the free-carrier density in Fig. 6 arise from different physical processes with different activation energies. The critical field which supplies the free electron with given activation energy to interact with impurities or defects is calculated with the equation of the hot

electron energy. The experimental critical field for each region of $n(E)$ characteristic of sample 1 in Fig. 6 is compared with the calculated result to verify the physical mechanism for the change of free-electron density.

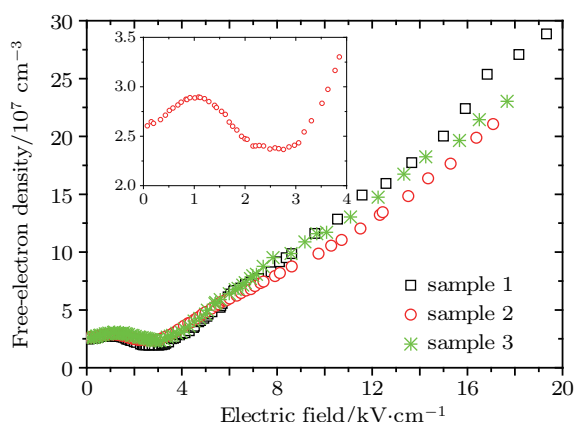


Fig. 6. (color online) Variations of free-electron density with electric field for three measured PCSSs. The inset shows the free-electron density of sample 2 at low field.

3.2.2. Critical field

At room temperature, the activation energy for the common impurity in GaAs is about 0.006 eV. Based on the free-electron energy at low field, the critical field which makes the impurities ionized in SI-GaAs should be greater than 500 V/cm. In Fig. 6 the initial field for the increase of free-carrier concentration is about 494 V/cm, which accords well with the calculated result.

When the energy of the hot electron is about 60 meV, which is gained from the field about 1 kV/cm, an additional density of states is introduced into the conduction band. Subsequently, the hot electron can be transferred from the conduction band to the trapped states of EL2, which leads to the field-enhanced capture of EL2 level.^[19] The trapping coefficient of EL2 increases to the maximum of about 3 kV/cm, after which it decreases slowly.^[20,21] Keeping in step with the field-dependent capture of EL2, the free-carrier concentration begins to reduce about 0.94 kV/cm and arrives at a minimum at 3 kV/cm (see Fig. 6).

Reaching its minimum at 3 kV/cm, the density of free carrier in Fig. 6 begins to increase subsequently. This may result from the competition between two effects, i.e., field-dependent trapping of EL2 and impact ionization of hot electrons with donor centers EL10 in SI-GaAs.^[22] The activation energy of EL10 centers with concentration 10^{15} cm^{-3} is 0.16 eV. Thus, the hot electron needs to gain enough energy from the field greater than 2.16 kV/cm to collide with the donor centers to release the carrier. However, the free-carrier density does not increase until 3 kV/cm, because the enhanced capture of EL2 dominates the density of the free carrier before 3 kV/cm. After that, the ionization of EL10 centers and the reduction of

the capture coefficient together lead to the increase of the free-carrier concentration with field increasing. It is interesting to note that the dark resistance in Fig. 5 does not start to decrease at 3 kV/cm but stays saturated till 3.14 kV/cm. This saturation is due to the compromise between the increase of the free carrier concentration and the decrease of electron mobility, which is confirmed by the constant result of the electron-density multiplied by the mobility in this region.

At room temperature, the activation energy of EL2 donor is about 0.688 eV,^[23] so the defect of EL2 can be involved in the impact ionization with field about 6.97 kV/cm, according to the equation of hot-electron energy. Note that there are differences among three samples in Fig. 6 at the field about 7 kV/cm, and the concentrations of free carrier begin to increase rapidly with the field increasing from 7 kV/cm. All of the fitting curves of $n(E)$ characteristics in the region above 7 kV/cm are exponential curves, as shown by the fitting curve of sample 1 in Fig. 7, which implies that the free carrier density will start to increase more rapidly from the field above 19.3 kV/cm. Under higher field, the electron mobility almost no longer decreases, so the rapid increase in leakage current always comes with the fast increase in free-carrier density. In pulsed-power applications, the field biased to the PCSS before triggering is always higher than the largest field of 19.3 kV/cm in this test. The lifetime of PCSS is inevitably degraded by the high leakage current. For this reason, the pulsed voltage source is always used for a high-power application of PCSS. Our measurement has not yet been carried out with a higher voltage on account of the lifetime of PCSS.

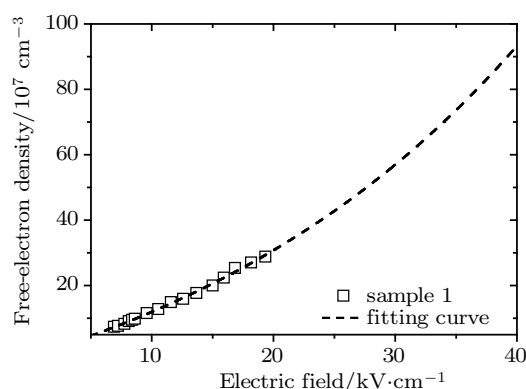


Fig. 7. Fitting curve for the last region of $n(E)$ characteristic for sample 1.

The experimental $J(E)$ characteristic is obtained by the present data from Eq. (5). Furthermore, the fitting curve of $J(E)$ can be achieved from the analytical expression in Ref. [24] by considering all of the five critical fields mentioned above. Here the current density J is expressed as a function of electric field E

$$J(E) = E \left(n_0 q \mu_0 + a \exp \left(\frac{-E_{c1}}{E} \right) \right)$$

$$-b \exp\left(\frac{-E_{c2}}{E}\right) + c \exp\left(\frac{-E_{c3}}{E}\right) + d \exp\left(\frac{-E_{c4}}{E}\right) + e \exp\left(\frac{-E_{c5}}{E}\right), \quad (7)$$

where $E_{c1} = 0.49$ kV/cm, $E_{c2} = 0.94$ kV/cm, $E_{c3} = 2.16$ kV/cm, $E_{c4} = 3.00$ kV/cm, and $E_{c5} = 6.97$ kV/cm are experimental critical fields from the physical mechanisms mentioned above, the parameters of a , b , c , d , and e are the fitting coefficients. Only the field-enhanced trapping with critical field E_{c2} reduces the current. The agreement between the fitting curve and experimental result in Fig. 8 shows that the leakage current is associated with these field-dependent physical processes.

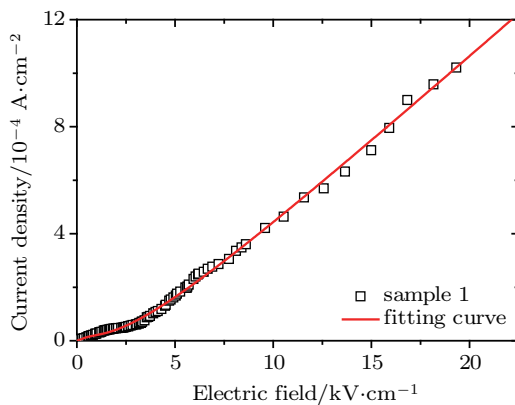


Fig. 8. (color online) Measured $J(E)$ characteristics and its fitting curve for sample 1.

For the SI-GaAs PCSS, the change shape of the free-carrier density in linear mode almost duplicates the shape in the dark state.^[25] The findings indicate that biased voltage has an effect on the PCSS no matter whether it is subject to optical illumination. The dark resistance even grows under the low voltage, so it is impossible to realize high gain when the charged PCSS is triggered by optical pulse into linear mode. The concentration of free-carriers increases with the increase of field which is higher than 3 kV/cm, especially 7 kV/cm, which is nearly the threshold field for the lock-on mode of the PCSS used. Additionally, as is well known, the optical energy needed to trigger PCSS into lock-on mode is inversely related to the increased field. It can be suggested that, first, PCSS is charged with high voltage to gain carrier multiplication, and then high gain is exhibited by optical excitation with the high field domain.^[26]

4. Conclusions

In this work, the effects of the voltage on the dark-state current and resistance of SI-GaAs PCSS are embodied in the variation of free-electron density. It can be found that the increase in the free-electron density is more rapid than the de-

crease in the dark resistance. The free-electron density increases exponentially with the field above 7 kV/cm, which will lead to the rapid increase in the leakage current with the higher field, and then the rapid degradation in lifetime. For each turning point of the $n(E)$ characteristic, the experimental critical fields keep in good agreement with the calculated results from the suggested physical processes. Furthermore, those physical processes are confirmed again by the agreement between the fitting curve and experimental data of $J(E)$ characteristics. These field-dependent physical processes in the dark states may give us an insight into the physical mechanism of PCSS.

Acknowledgment

Authors would like to thank Prof. Jiu-Xun Sun and Dr. Ya-Chun Gao for their help and advice.

References

- [1] Wang W, Xia L, Chen Y, Liu Y, Yang C, Ye M and Deng J 2015 *Appl. Phys. Lett.* **106** 022108
- [2] Zutavern F J, Loubriel G M, O'Malley M W, Shanwald L P, Helgeson W D, McLaughlin D L and McKenzie B B 1990 *IEEE Trans. Electr. Dev.* **37** 2472
- [3] Shi W, Zhang Z and Hou L 2010 *Chin. Phys. Lett.* **27** 087203
- [4] Zhang T, Liu K, Gao S and Shi Y 2015 *IEEE Trans. Dielectr. Electr. Insul.* **22** 1191
- [5] Shi W, Jiang H, Li M, Ma C, Gui H, Wang L, Xue P, Fu Z and Cao J 2014 *Appl. Phys. Lett.* **104** 042108
- [6] Zutavern F J, Loubriel G M, McLaughlin D L, Helgeson W D and O'Malley M W 1992 *SPIE* **1632** 152
- [7] Lin G R and Pan C L 2000 *Opt. Quant. Electron.* **32** 553
- [8] Zheng X, Fan S, Chen Y, Kang D, Zhang J, Wang C, Mo J, Li L, Ma X, Zhang J and Hao Y 2015 *Chin. Phys. B* **24** 027302
- [9] Li W, Liu D and Zhang H 2014 *Acta Phys. Sin.* **63** 227303 (in Chinese)
- [10] Davanloo F, Collins C B and Agee F J 2002 *IEEE Trans. on Plasma Sci.* **30** 1897
- [11] Adams J C, Falk R A, Capps C D and Ferrier S 1992 *SPIE* **1632** 110
- [12] Saxce T D 1992 *SPIE* **1632** 167
- [13] Zamdmer N, Hu Q, McIntosh K A and Verghese S 1999 *Appl. Phys. Lett.* **75** 2313
- [14] Wang B, Liu K and Qiu J 2013 *IEEE Trans. Dielectr. Electr. Insul.* **20** 1287
- [15] Amari S E, Angelis A D, Arnaud-cormos D, Couderc V and Leveque P 2011 *IEEE Photon. Tech. Lett.* **23** 673
- [16] Yang H, Cui H and Wu M 2010 *Chinese Sci. Bull.* **55** 1331
- [17] Sze S M 2007 *Transferred-electron Devices in Physics of Semiconductor Devices*, 3rd ed. (Hoboken: Wiley) pp. 511–516
- [18] Kroemer H 1967 *IEEE Trans. Electron Dev.* **14** 476
- [19] Kaminska M, Parsey J M, Lagowski J and Gatos H C 1982 *Appl. Phys. Lett.* **41** 989
- [20] Willing B and Maan J C 1996 *J. Phys.: Condens. Matter* **8** 7493
- [21] Pizza F, Christianen P C M and Maan J C 1996 *Appl. Phys. Lett.* **69** 1909
- [22] Paracchini C and Dallacasa V 1989 *Solid State Commun.* **69** 49
- [23] Look D C and Fang Z Q 1999 *Solid State Electron.* **43** 1317
- [24] Albuquerque H A, Oliveira A G de, Ribeiro G M, Silva R L da, Rodrigues W N, Moreira M V B and Rubinger R M 2003 *J. Appl. Phys.* **93** 1647
- [25] Cui H, Yang H, Xu J, Yang Z and Yang Y 2016 *IEEE Electron. Device Lett.* Accepted
- [26] Shi W and Ma X 2011 *Chin. Phys. Lett.* **28** 124201